

# Stability and topological nature of charged Gauss–Bonnet AdS black holes in five dimensions

Imtak Jeon<sup>a,b</sup>, Bum-Hoon Lee<sup>c,d</sup>, Wonwoo Lee<sup>c</sup> and Madhu Mishra<sup>a</sup>

<sup>a</sup> *Asia Pacific Center for Theoretical Physics, Postech, Pohang 37673, Korea*

<sup>b</sup> *Department of Physics, Postech, Pohang 37673, Korea*

<sup>c</sup> *Center for Quantum Spacetime, Sogang University, Seoul 04107, Republic of Korea*

<sup>d</sup> *Department of Physics, Sogang University, Seoul 04107, Republic of Korea*

E-mail: imtakjeon@gmail.com, bhl@sogang.ac.kr, warrior@sogang.ac.kr, madhu.mishra@apctp.org

## Abstract

We examine the thermodynamic characteristics and phase structures of a black hole, where the black hole horizon could be a hypersurface with positive, zero, or negative constant curvature, within the framework of Einstein-Maxwell theory, incorporating a negative cosmological constant and a Gauss-Bonnet (GB) correction. Our research follows the topological approach to black hole thermodynamics where we treat anti-de Sitter (AdS) black holes as topological defects in thermodynamic space. We study the nature of the black hole's critical points and local stability by computing the winding numbers/topological charge associated with the zero point of the vector field, derived from the temperature of extremal points and the generalized off-shell Gibbs free energy, respectively. Black holes are classified into different topological classes based on their topological number. In this study, we found unlike the charged AdS black hole, the charged GB AdS black hole exhibits a critical point. Our findings reveal the occurrence of a liquid/gas-like first-order phase transition between small-large black hole phases of the spherical charged GB AdS black hole. We conclude that the charged GB AdS and charged AdS black holes belong to different topological classes in the grand canonical ensemble. Furthermore, connecting with the previous studies, we conclude that the charged AdS and charged GB AdS black holes in canonical and charged GB in the grand canonical ensemble belong to the same topological classes.

# Contents

<b>1</b>	<b>Introduction</b>	<b>2</b>
<b>2</b>	<b>Charged AdS black holes in Einstein–Gauss-Bonnet gravity</b>	<b>7</b>
<b>3</b>	<b>Topological natures of the charged Gauss-Bonnet black hole in AdS space</b>	<b>8</b>
3.1	Topology of charged Gauss-Bonnet AdS black hole thermodynamics in grand canonical ensemble . . . . .	9
3.2	Charged Gauss-Bonnet AdS black hole thermodynamics as topological defects in grand canonical ensemble . . . . .	12
3.2.1	$k = 0$ . . . . .	14
3.2.2	$k = 1$ . . . . .	15
3.2.3	$k = -1$ . . . . .	18
<b>4</b>	<b>Stability and Phase transition of RN GB Topological Black Holes</b>	<b>18</b>
4.1	Local Stability . . . . .	20
4.1.1	$k = 0$ . . . . .	21
4.1.2	$k = 1$ . . . . .	22
4.1.3	$k = -1$ . . . . .	23
4.2	Phase Transition . . . . .	23
4.2.1	$k = 0$ . . . . .	26
4.2.2	$k = 1$ . . . . .	27
4.2.3	$k = -1$ . . . . .	29
<b>5</b>	<b>Conclusion</b>	<b>30</b>

## 1 Introduction

For decades, black hole thermodynamics has piqued curiosity among scientists. The Hawking-Page phase transition between the phase spaces of the Schwarzschild AdS black hole and pure AdS space was demonstrated in [1]. Subsequently, several more complex backgrounds have since been investigated in other ensembles, including the Gauss-Bonnet(GB) AdS black holes, charged (Reissner-Nordstrom RN) and RN-GB AdS black holes [2–9]. In the canonical ensemble with fixed black hole charge, the phase transition between small and large black holes

occurs in charged AdS black holes with or without Gauss-Bonnet corrections. The subject has been expanded to include the grand canonical ensemble, which allows the black hole to emit and absorb charged particles while maintaining a constant potential until thermal equilibrium is established. In the grand canonical ensemble, no critical behavior is seen for the spherical RN AdS black hole [2–4]. The phase transition between the small and large black holes in the grand canonical ensemble can still occur for the spherically RN-GB AdS black hole in five dimensions [6–8].

Thermodynamic topology has recently been introduced into the study of criticality and stability in black holes. The introduction of topology into the study of black hole thermodynamics was first initiated in [10], by using Duan’s topological current  $\phi$ -mapping theory [11] in the thermodynamic space of a black hole. While critical points have been well studied in phase transition research, the study in [10] highlighted two distinct kinds of critical points that were previously overlooked. Since entropy and temperature are known to exist in any black hole, the universal conditions one chooses to determine the critical point are as follows

$$\left(\frac{\partial T}{\partial r_+}\right)_{P,z^i} = 0 \quad \text{and} \quad \left(\frac{\partial^2 T}{\partial r_+^2}\right)_{P,z^i} = 0. \quad (1.0.1)$$

The temperature  $T(P, r_+, z^i)$  of a black hole in extended thermodynamic space is described as a function of pressure, horizon radius, and other parameters. To analyze the criticality, the authors in [10], define a thermodynamic function  $\Phi$ , known as Duan’s potential as

$$\Phi = \frac{1}{\sin \theta} T(r_+, z^i). \quad (1.0.2)$$

where pressure  $P$  has been eliminated by using the condition  $\left(\frac{\partial T}{\partial r_+}\right)_{P,z^i} = 0$  and an additional factor  $1/\sin \theta$  is introduced for the ease of analysis. We define a two-dimensional vector  $\phi = (\phi^{r_+}, \phi^\theta)$  as

$$\phi^{r_+} = (\partial_{r_+} \Phi)_{\theta, z^i} \quad , \quad \phi^\theta = (\partial_\theta \Phi)_{r_+, z^i}. \quad (1.0.3)$$

Based on the criteria (1.0.1), the critical points of a black hole in the thermodynamic space are identified with the zero point of the vector field  $\phi$ , i.e.,  $\phi^a(z^i) = 0$ . To verify, we refer to the appendix of [10]. This trait enables us to explore the critical point of a black hole using topology. In the framework of Duan’s  $\phi$ -mapping [11], the topological current is defined in terms of the unit vector  $n^a = \frac{\phi^a}{\|\phi^a\|}$  ( $a = r_+, \theta$ ) as

$$j^\mu = \frac{1}{2\pi} \epsilon^{\mu\nu\rho} \epsilon_{ab} \partial_\nu n^a \partial_\rho n^b, \quad (1.0.4)$$

where  $x^\mu = (t, r_+, \theta)$ . It is interesting to notice that the presence of  $\theta$  in the Duan's potential (1.0.2) ensures that the zero point of the vector field  $\phi$  is always at  $\theta = \pi/2$ .

This framework guarantees the presence of a topological charge, which for a given parameter space  $\Sigma$  is equivalent to

$$Q_t = \int_{\Sigma} j^0 d^2x = \sum_{i=1}^N w_i. \quad (1.0.5)$$

The variables denoted by  $w_i$  and  $j^0$  represent the winding number of the  $i$ -th zero point of  $\phi$  and the topological current density, respectively. A winding number is a mathematical notion that describes how many times a curve wraps around a point in a plane. The topological charge  $Q_t$  is an integer given by the sum of the winding number of a vector field  $\phi$  around the critical point. The critical points with topological charges of  $-1$  and  $+1$ , have different topological properties and are described as conventional critical points and novel critical points, respectively. For the detailed construction of topological charge please follow [10]. It was asserted in [10] that a first-order phase transition is not present at critical points with a topological charge of  $Q_t = +1$ . Conversely, conventional critical points exhibiting a topological charge of  $Q_t = -1$  can be thought to possess a first-order phase transition. However, in a certain parameter regime, this relationship between the occurrence of first-order phase transitions and the topological nature of critical points breaks down. Thus, as a resolution in [12], it was suggested that the novel and conventional critical points should be treated as phase creation and annihilation points, respectively.

Inspired by the above construction, in [13], authors employ generalized off-shell free energy (mass and temperature are independent variables) [14] as Duan's potential. In the grand canonical ensemble, the generalized Gibbs free energy  $\mathcal{G}$  is given as

$$\mathcal{G} = M - \frac{S}{\tau} - \varphi Q = \mathcal{G}(r_+, \tau, \varphi), \quad (1.0.6)$$

where  $S$  is the entropy,  $Q$  is the charge and  $\varphi$  is the electric potential. Here,  $\tau$  represents the inverse of the ensemble temperature which is independent of mass/enthalpy  $M$ , while we choose the  $\varphi$  to be an on-shell value of chemical potential for the charge  $Q$ <sup>1</sup>. The extremal

---

<sup>1</sup>In the extended phase space, the thermodynamic quantities satisfy the first law of the black hole thermodynamic as follows

$$dM = TdS + \varphi dQ + VdP + Ad\alpha$$

$$T = \left( \frac{\partial M}{\partial S} \right)_{P, Q, \alpha}, \quad V = \left( \frac{\partial M}{\partial P} \right)_{S, Q, \alpha}, \quad \mathcal{A} = \left( \frac{\partial M}{\partial \alpha} \right)_{S, Q, P},$$

points of the generalized free energy  $\mathcal{G}$  are determined by imposing [15]

$$\left(\frac{\partial\mathcal{G}}{\partial r_+}\right)_{P,\varphi,\tau,\alpha} = 0. \quad (1.0.7)$$

The equation (1.0.7) is the on-shell condition for the generalized free energy. The ensemble temperature at the extreme points of  $\mathcal{G}$  is equal to the Hawking temperature  $\tau^{-1} = T$ , which can be seen from the first law in the footnote.

$$\left(\frac{\partial M}{\partial S}\right)_{P,Q,\alpha} = \tau^{-1} = T. \quad (1.0.8)$$

The black hole solution is an on-shell (which satisfies Einstein's equations of motion). A vector field  $\phi$  is defined from  $\mathcal{G}$  in the following way:

$$\phi = \left(\frac{\partial\mathcal{G}}{\partial r_+}, -\cot\Theta \csc\Theta\right). \quad (1.0.9)$$

The zero point of the vector  $\phi$  corresponds to  $\Theta = \pi/2$  and extremal points of  $\mathcal{G}$ . This confirms that the zero point of a vector  $\phi$  which is generally called defects, meets the black hole solution exactly. These defects are then analyzed in terms of their winding numbers which is the most basic topological quantity connected to a zero point of a field. The winding number corresponding to vector (1.0.9) is related to  $sign\left(\frac{\partial^2\mathcal{G}}{\partial r_+^2}\right)|_{z_i}$  (See Appendix in [16] for details). Consequently, we may use  $\phi$  from a topological perspective to investigate the local stability and global features of the black holes.

*Local properties* : There exists a connection between the thermodynamic stability<sup>2</sup> of the appropriate black hole solution and the sign of the winding number of defects. The winding numbers reflect the local topological natures; the stable and unstable black hole branches are represented by positive and negative winding numbers, respectively.

---

where  $V$  is the thermodynamic volume, the conjugate variable of the pressure  $P$  and  $\mathcal{A}$  denote the conjugate Gauss-Bonnet parameter  $\alpha$  and while the mass obtains a new physical meaning, the enthalpy  $M \equiv H$  rather than the energy of the system.

<sup>2</sup>The Hawking-Page (HP) phase transition represents the transition occurring between the AdS black hole and the thermal AdS space. The description of the phase transition is based on the free energy difference, in which the Helmholtz free energy vanishes for the thermal AdS space with spherical symmetry in the canonical ensemble [1]. In black hole thermodynamics, local stability is determined by the sign of the specific heat (or heat capacity), while global stability is determined by the sign of the difference in the free energy between two systems. In other words, which one is more probable? The charge and the temperature are specified at the boundary in the canonical ensemble, while the electrostatic potential and the temperature are specified in the grand canonical ensemble [2]. The HP phase transition has been extensively studied in various theories of gravitation [3, 17–25].

*Topological classes:* The topological numbers, which can be used to categorize black holes into distinct classes, are defined as the total of the winding numbers for each black hole branch. These numbers reflect the global topological natures of the black holes.

In [16], the authors investigated the local and global topological properties of the charged Gauss-Bonnet black hole in AdS space in a canonical ensemble. The study found that higher derivatives of curvature, such as Gauss-Bonnet gravity, do not affect the topological number in five dimensions. It was also discovered that the topological number was unaffected by the black hole horizon's geometry. Due to charge conservation, a black hole in the canonical ensemble with a fixed charge cannot transition from an RN black hole (charged phase) to an electrically neutral thermal AdS space. To examine the Hawking-Page phase transitions of RN-GB AdS black holes one needs to examine the phase structure of black holes in the grand canonical ensemble, in which the electric charge is variable but the electric potential is fixed. In [26,27], authors chose order parameters to be  $r_+$  and  $Q$  to study the topology of the landscape of RN-GB AdS black hole in a grand canonical ensemble. They agree that the topological defect of the gradient field can be treated as a black hole as proposed in [13], but they argue that the stability is not necessarily related to the winding number of these zero points.

In this work, we extend the study of thermodynamic topology to RN-GB black holes in the grand canonical ensemble, in parameter space  $r_+$  and  $\Theta$  as originally proposed in [13]. For this parameter space, we find that the local stability of the black hole is related to the sign of the winding number. We also find that in the grand canonical ensemble, the presence of GB correction plays a crucial role in the study of critical points, and it was discovered that the topological numbers for RN AdS and RN-GB AdS black holes differ. In [28], it was shown that the topological number in the grand canonical ensemble is different from that in the canonical ensemble for the charged AdS black hole system. We show for the RN-GB AdS black hole that the topological number is the same for the grand canonical and the canonical ensemble.

The paper has been structured as follows. In section 2, we review charged Gauss-Bonnet AdS black holes in five dimensions and give their thermodynamic properties in the extended phase space. In section 3, we analyze the topological thermodynamics of black holes in the grand canonical ensemble. We locate critical points and categorize the formation of thermodynamic phases and phase transitions based on horizon geometry. In section 4, we look at the local stability of the RN-GB AdS black holes in the grand canonical ensemble by explicitly computing their specific heat and analyzing phase transitions using Gibbs free energy versus temperature plots. Finally, we conclude in section 5.

## 2 Charged AdS black holes in Einstein–Gauss-Bonnet gravity

The Einstein-Maxwell Gauss–Bonnet action in five dimensions is given by [29, 30]

$$S = \frac{1}{16\pi} \int d^5x \sqrt{-g} \left( R - 2\Lambda + \frac{\alpha}{2} (R_{\mu\nu\rho\sigma} R^{\mu\nu\rho\sigma} - 4R_{\mu\nu} R^{\mu\nu} + R^2) - 4\pi F_{\mu\nu} F^{\mu\nu} \right) + S_b, \quad (2.0.1)$$

where  $\Lambda$  is the cosmological constant expressed in terms of AdS radius  $\ell$ , as  $\Lambda = -6\ell^{-2}$ ,  $\alpha$  is the Gauss-Bonnet coefficient with dimension  $(length)^2$  and  $S_b$  is the boundary term [31–34]. In this work, we restrict ourselves to the cases where  $\alpha \geq 0$ . The most general known black hole solution to this theory is given by the charged Gauss-Bonnet asymptotically AdS<sub>5</sub> black holes as

$$ds^2 = -f(r)dt^2 + f^{-1}(r)dr^2 + r^2 d\Omega_3^2. \quad (2.0.2)$$

The  $d\Omega_3^2$  components of the line element denote a 3d hypersurface. The asymptotically AdS spaces include black holes with event horizons with zero or negative constant curvature hypersurfaces and spherically symmetric black holes for which the curvature constant is positive. In the literature, these black holes are referred to as topological black holes with

$$f(r) = k + \frac{r^2}{2\alpha} \left( 1 - \sqrt{1 + \frac{32\alpha M}{3\pi r^4} - \frac{16\alpha Q^2}{3\pi^2 r^6} - \frac{4\alpha}{l^2}} \right), \quad (2.0.3)$$

where  $k$  represents constant curvatures for  $k = -1, 0, +1$  we have black horizon have hyperbolic, planar, and spherical geometry, respectively. Recent research has focused on determining criticality in AdS black holes in extended thermodynamic space [35]. The understanding that the negative cosmological constant causes positive vacuum pressure in spacetime entails employing the cosmological constant  $\Lambda$  as the thermodynamic pressure  $P$  [36–39]

$$P = -\frac{\Lambda}{8\pi} = \frac{3}{4\pi\ell^2}. \quad (2.0.4)$$

Thus, we present the list of thermodynamic quantities in terms of pressure  $P$ , black hole charge  $Q$ , and horizon radius  $r_+$ , which is given by the largest positive root of the metric function

$$f(r)|_{r=r_+} = 0$$

$$M = \frac{\pi}{8} (3kr_+^2 + 4\pi Pr_+^4 + 3\alpha k^2) + \frac{Q^2}{2\pi r_+^2}, \quad (2.0.5)$$

$$T = \frac{\pi^2 r_+^4 (8\pi Pr_+^2 + 3k) - 4Q^2}{6\pi^3 r_+^3 (r_+^2 + 2k\alpha)}, \quad (2.0.6)$$

$$S = \frac{\pi^2 r_+^3}{2} \left( 1 + \frac{6k\alpha}{r_+^2} \right), \quad (2.0.7)$$

$$\varphi = \frac{Q}{\pi r_+^2}, \quad V = \frac{\pi^2}{2} r_+^4, \quad \mathcal{A} = \frac{3\pi^2}{8} k^2, \quad (2.0.8)$$

where  $V$  and  $\mathcal{A}$  denote the conjugate of  $P$  and  $\alpha$ . The chemical potential  $\varphi$  specifies the conjugate quantity of the charge  $Q$ . It is important to note that the Gauss-Bonnet parameter  $\alpha$  is always accompanied by constant curvature  $k$  thus for  $k = 0$  thermodynamic quantities do not get affected by the presence of the Gauss-Bonnet term. We should also keep in mind that certain limits need to be satisfied for a well-defined solution. For  $\alpha > 0$ , the first constraint comes from the metric function (2.0.3), where a well-behaved vacuum solution  $M = Q = 0$  requires

$$0 \leq P \leq \frac{3}{16\pi\alpha}. \quad (2.0.9)$$

Another requirement is the non-negative definiteness of the black hole entropy (2.0.7) [40, 41], which demands <sup>3</sup>

$$(r_+^2 + 6k\alpha) \geq 0. \quad (2.0.10)$$

From (2.0.10), we infer that the spherical and planar horizon curvatures allow for all the positive values of horizon radius. However, for hyperbolic horizon curvature ( $k = -1$ ), the horizon radius is bounded from below <sup>4</sup>. Keeping the constraints in mind we will study the topological thermodynamics for all three geometries in the following section [Sec.3].

### 3 Topological natures of the charged Gauss-Bonnet black hole in AdS space

In subsection 3.1, we investigate the critical points of the RN-GB AdS black holes in the grand canonical ensemble following the analysis in [10] and categorize the nature of critical points

---

<sup>3</sup>We do not consider the possibility of adding an ambiguity to redefine the entropy [42].

<sup>4</sup>This result will be interchanged between spherical and hyperbolic geometry for  $\alpha < 0$ .



based on the sign of their topological charge [43]. In subsection 3.2, we follow [13], and consider the generalized free energy in grand canonical ensemble to study the local stability of black hole phase based on the sign of their winding and in the end, investigate the topological class of the RN-GB AdS black hole in the grand canonical ensemble based on their topological number.

### 3.1 Topology of charged Gauss-Bonnet AdS black hole thermodynamics in grand canonical ensemble

In a grand canonical ensemble, the temperature  $T$  of RN-GB AdS black hole as a function of pressure  $P$ , horizon radius  $r_+$ , and electric potential  $\varphi$  is given by

$$T = \frac{8\pi P r_+^3 + (3k - 4\varphi^2) r_+}{6\pi(r_+^2 + 2k\alpha)}. \quad (3.1.1)$$

In this approach, one first calculates the extremal points of the temperature. Using the condition  $\left(\frac{\partial T}{\partial r_+}\right)_{P,\varphi} = 0$ , this yields an expression for pressure given as,

$$P = \frac{(3k - 4\varphi^2)(r_+^2 - 2k\alpha)}{8\pi r_+^2(r_+^2 + 6k\alpha)}. \quad (3.1.2)$$

Plugging  $P$  in (3.1.1), we obtain the temperature  $T(r_+, z^i)$  of these extremal points. Now using the definition (1.0.2) of Duan's potential, we get

$$\Phi = \frac{r_+ \csc \theta (3k - 4\varphi^2)}{3\pi(r_+^2 + 6k\alpha)}. \quad (3.1.3)$$

The vector components of the vector field  $\phi = (\phi^{r_+}, \phi^\theta)$  are obtained as

$$\phi^{r_+} = \left(\frac{\partial \Phi}{\partial r_+}\right)_{\varphi,\theta} = -\frac{(r_+^2 - 6k\alpha)(3k - 4\varphi^2) \csc \theta}{3\pi(r_+^2 + 6k\alpha)}, \quad (3.1.4)$$

$$\phi^\theta = \left(\frac{\partial \Phi}{\partial \theta}\right)_{\varphi,r_+} = -\frac{r_+(3k - 4\varphi^2) \cot \theta \csc \theta}{3\pi(r_+^2 + 6k\alpha)}. \quad (3.1.5)$$

The normalized vector components are given by the unit vector  $n^a = \frac{\phi^a}{\|\phi^a\|}$  as

$$n^1 = \frac{\phi^{r_+}}{\sqrt{(\phi^\theta)^2 + (\phi^{r_+})^2}} = -\frac{r_+^2 - 6k\alpha}{\sqrt{r_+^2 \cot^2 \theta (r_+^2 + 6k\alpha)^2 + (r_+^2 - 6k\alpha)^2}}, \quad (3.1.6)$$

$$n^2 = \frac{\phi^\theta}{\sqrt{(\phi^\theta)^2 + (\phi^{r_+})^2}} = -\frac{r_+(r_+^2 + 6k\alpha) \cot \theta}{\sqrt{r_+^2 \cot^2 \theta (r_+^2 + 6k\alpha)^2 + (r_+^2 - 6k\alpha)^2}}. \quad (3.1.7)$$

The critical points are determined by setting  $\theta = \pi/2$  and equating (3.1.4) to zero. The critical point is at  $(r_c, \theta) = (\sqrt{6k\alpha}, \pi/2)$ , which exactly matches with the critical points obtained by (1.0.1). It also agrees with the study in [8] that the RN-AdS black holes in the extended phase space do not exhibit criticality in the grand canonical ensemble which can be checked by taking  $\alpha$  going to zero limit<sup>5</sup>. The critical pressure and the critical temperature for  $r_c = \sqrt{6k\alpha}$  are given as,

$$P_c = \frac{3k - 4\varphi^2}{144\pi\alpha k} \quad \text{and} \quad T_c = \frac{3k - 4\varphi^2}{6\pi\sqrt{6k\alpha}}. \quad (3.1.8)$$

- We conclude from the critical expressions of  $T_c$ ,  $P_c$  and  $r_c$ , that no critical points were found for  $k = 0$  case.
- It is also evident that there cannot be a physical solution for  $r_c$  for  $k = -1$ . This means that the black hole horizon with hyperbolic geometry does not have a critical point.
- For  $k = 1$  and  $\alpha > 0$ ,  $r_c$  is independent of the choice of potential. However, for potential  $\varphi = \sqrt{3}/2$ , the critical temperature  $T_c$  and  $P_c$  both disappear and become negative for  $\varphi > \sqrt{3}/2$ .
- In conclusion, RN-GB AdS black holes in a grand canonical ensemble show critical behavior for spherical geometry within the potential range  $0 \leq \varphi \leq \frac{\sqrt{3}}{2}$ .

*Nature of critical point:* Depending on the sign of the topological charge  $Q$ , there are two different kinds of critical points from the topology, as seen in [10, 43]. Whereas the novel critical point has  $Q = 1$ , the conventional one has  $Q = -1$ . To determine the topological charge of a critical point (where  $\phi^a = 0$ ), we compute its winding number ( $w_i$ ) by measuring the deflection  $\Omega(\vartheta)$  of the vector field  $\phi$  along the given contour as

$$Q_t = \frac{1}{2\pi} \Omega(2\pi), \quad (3.1.9)$$

where

$$\Omega(\vartheta) = \int_0^{\vartheta} \epsilon_{ab} n^a \partial_{\vartheta} n^b d\vartheta. \quad (3.1.10)$$

---

<sup>5</sup>In the canonical ensemble, however, there exists a critical point in this limit given as

$$r_c = \frac{\sqrt{2} \sqrt[4]{5} \sqrt{Q}}{\sqrt{\pi} \sqrt[4]{k}}.$$

Following [10], we choose a contour  $C$  to be an ellipse centered at  $(r_c, \frac{\pi}{2})$  parameterized by the angle  $\vartheta \in (0, 2\pi)$

$$\begin{cases} r_+ = c \cos \vartheta + r_c, \\ \theta = d \sin \vartheta + \frac{\pi}{2}. \end{cases} \quad (3.1.11)$$

The critical point  $CP_1$  is enclosed by the first contour  $C_1$ , whereas the second contour  $C_2$  is outside of the critical point. In Figure 1, We show critical point for  $\alpha = 0.05$ . For computing the topological charge for this critical point, we choose  $(c, d, r_c) = (0.3, 0.2, \sqrt{0.3})$  and  $(0.4, 0.4, 2)$  for contours  $C_1$  and  $C_2$ , respectively.

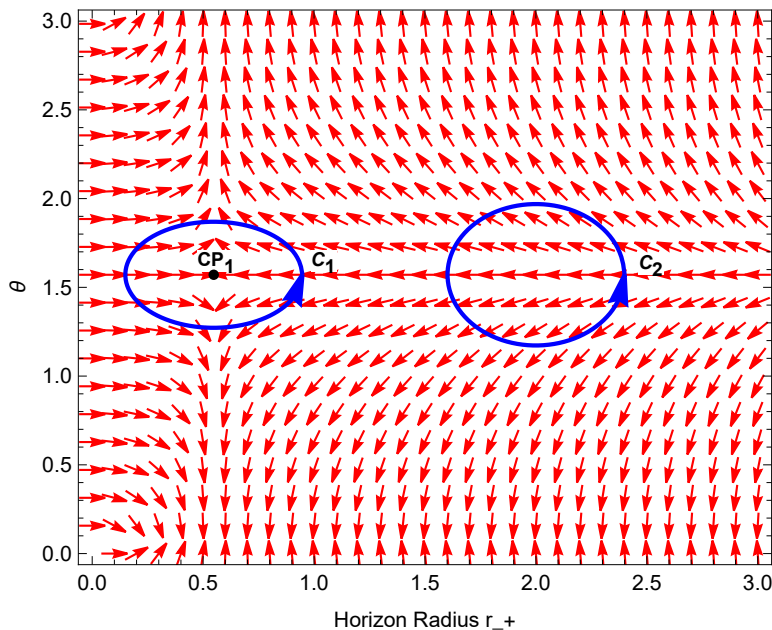


Figure 1: Plot of the normalized vector field  $n^a$  in  $r_+$  vs  $\theta$  plane for charged Gauss-Bonnet AdS black hole in the grand canonical ensemble. The black dot  $CP_1$  represents the critical point.

We found that for the critical point  $CP_1$  enclosed by the contour  $C_1$ , the topological charge is  $Q_{CP_1} = -1$  which means it is a conventional critical point. Since the contour  $C_2$  does not enclose any critical point, it corresponds to zero topological charge. Thus, the total topological charge is  $Q = -1$ . Thus, unlike RN AdS black hole, RN Gauss-Bonnet black exhibits one critical point in canonical as well as grand canonical ensemble. In Table 1, we provide the list of critical points and topological charges for different values of GB coupling parameter.

In Figure 2, we plot the  $T - r_+$  isobaric diagram for spherical RN-GB AdS black holes with  $\varphi = 0.5$  and  $\alpha = 0.05$ . It shows that each isobaric curve has two black hole phases for a pressure  $P < P_c$  lower than the critical value. On increasing the pressure, these two phases

Case		$C_1$	$C_2$	$Q_1$	$Q_2$	$Q$
$\alpha = 0$	c	0.07	0.07			
	d	0.4	0.4	0	0	0
	$r_c$	0.5	1			
$\alpha = 0.05$	c	0.3	0.4			
	d	0.2	0.4	-1	0	-1
	$r_c$	0.5577	2			
$\alpha = 0.5$	c	0.3	0.15			
	d	0.2	0.4	-1	0	-1
	$r_c$	1.732	1			

Table 1: Critical points and topological charge for various Gauss-Bonnet coupling in grand canonical ensemble.

coincide at the critical point  $CP_1$ , and we are left with only one black hole phase, beyond the critical pressure  $P > P_c$ . This is the reason the conventional critical points are classified as phase disappearing/annihilation points.

### 3.2 Charged Gauss-Bonnet AdS black hole thermodynamics as topological defects in grand canonical ensemble

Now we proceed to explore the five-dimensional charged Gauss-Bonnet AdS black hole solutions as topological thermodynamics defects in grand canonical ensemble. The generalized Gibbs free energy  $\mathcal{G}(\tau, r_+, P, \varphi)$  of an RN GB black hole in the grand canonical ensemble is given as

$$\mathcal{G} = \frac{\pi (4\pi (Pr_+^4\tau - r_+^3 - 6k\alpha r_+) + 3k\tau (r_+^2 + k\alpha) - 4r_+^2\tau\varphi^2)}{8\tau}. \quad (3.2.1)$$

When the ensemble temperature  $\tau^{-1}$  equals the Hawking temperature  $T$ , the on-shell black hole branches represent the extremal points in the Gibbs free energy (1.0.7). Following (1.0.9), the vector component yields

$$\phi^{r_+} = \frac{\pi (2\pi (4Pr_+^3\tau - 3r_+^2 - 6k\alpha) + r_+\tau (3k - 4\varphi^2))}{4\tau}, \quad (3.2.2)$$

$$\phi^\Theta = -\cot \Theta \csc \Theta, \quad (3.2.3)$$

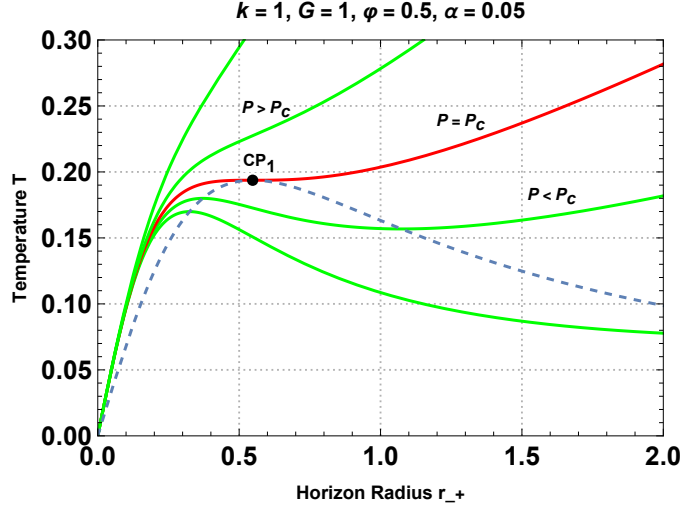


Figure 2: Isobaric curves (red and green) of charged Gauss-Bonnet AdS black hole in the grand canonical ensemble. The Blue dashed curve is for the extremal points of the temperature and the critical point is marked with a black dot.

and corresponding unit vectors are as follows,

$$n^1 = \frac{\pi(-6\pi(r_+^2 + 2k\alpha) + r_+\tau(3k - 4\varphi^2) + 8\pi Pr_+^3\tau)}{4\tau\sqrt{\cot^2\Theta \csc^2\Theta + \frac{\pi^2(\pi(12\alpha k - 8Pr_+^3\tau + 6r_+^2) + r_+\tau(4\varphi^2 - 3k))^2}{16\tau^2}}}, \quad (3.2.4)$$

$$n^2 = -\frac{\cot\Theta \csc\Theta}{\sqrt{\cot^2\Theta \csc^2\Theta + \frac{\pi^2(\pi(12\alpha k - 8Pr_+^3\tau + 6r_+^2) + r_+\tau(4\varphi^2 - 3k))^2}{16\tau^2}}}. \quad (3.2.5)$$

At the zero point  $\phi^{r_+} = 0$   $\Theta = \pi/2$ , the expression for  $\tau$  (inverse of black hole temperature) is obtained as

$$\tau = \frac{6\pi(r_+^2 + 2k\alpha)}{r_+(3k + 8\pi Pr_+^2 - 4\varphi^2)}. \quad (3.2.6)$$

In the following subsections, we will analyze the zero points and local stability for RN-GB AdS black hole solutions for the horizon of the black hole that has positive, negative curvature, or zero constant curvature hypersurface.

### 3.2.1 $k = 0$

We notice that the thermodynamic quantities, for  $k = 0$ , are interestingly independent of the Gauss-Bonnet parameter  $\alpha$ . For instance,

$$\tau = \frac{3\pi r_+}{2(2\pi P r_+^2 - \varphi^2)}, \quad (3.2.7)$$

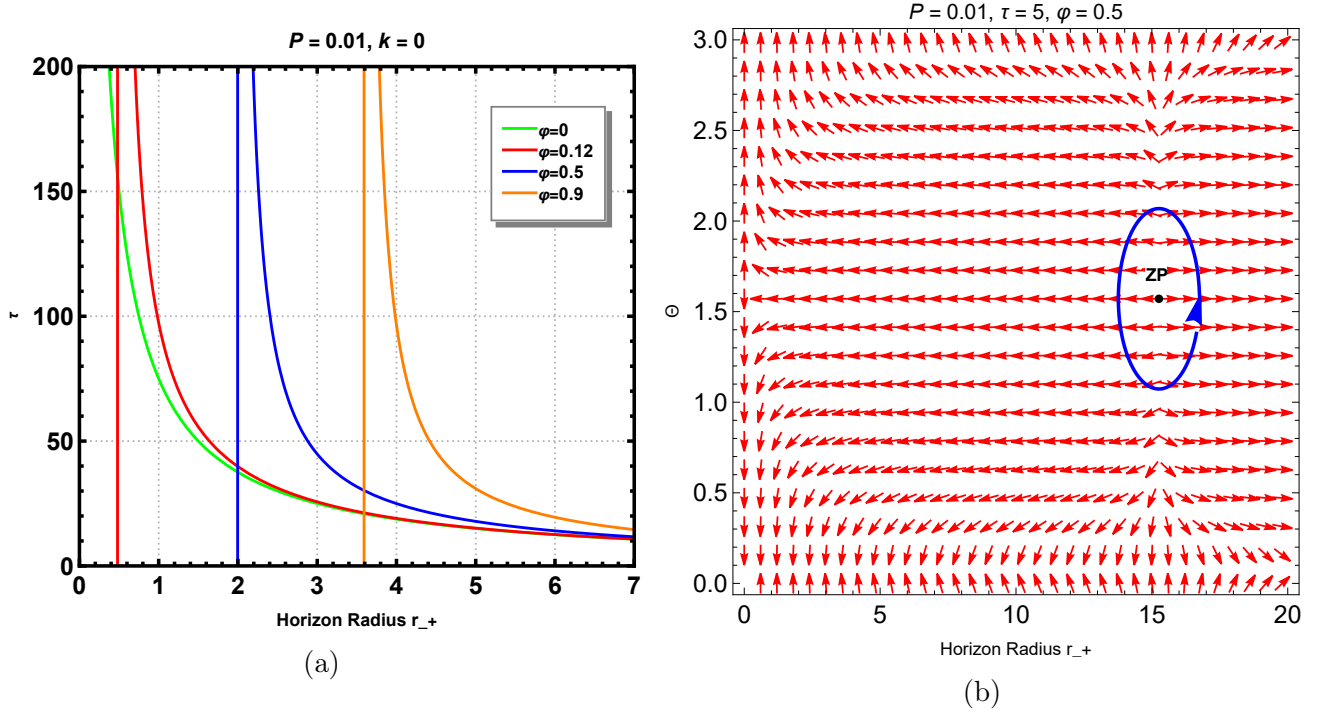


Figure 3: The zero points of  $\phi^{r_+}$  in (a)  $r_+ - \tau$  plane and (b)  $r_+ - \Theta$  plane, for charged AdS black hole in grand canonical ensemble with  $\tau = 5$ ,  $\varphi = 0.5$ , and pressure  $P = 0.01$ .

is independent of parameter  $\alpha$ . For  $k = 0$ , we get only one black hole branch with winding number  $+1$ . We repeated our analysis by changing the values of pressure  $P$  and found that the winding/topological number ( $+1$ ) does not get altered by varying pressure. As an example, we show in Figure 3, the zero points of  $\phi^{r_+}$  in  $r_+ - \tau$  plane and unit vectors in  $r_+ - \Theta$  plane for  $\tau = 5$ ,  $\varphi = 0.5$ , and pressure  $P = 0.01$ . This indicates that for case  $k = 0$ , the black holes are locally thermodynamically stable.

### 3.2.2 $k = 1$

For  $k = 1$ , we have a physical solution of  $r_c$  for non-zero Gauss-Bonnet coupling with positive critical temperature  $T_c$  and critical pressure  $P_c$  for the potential range  $0 \leq \varphi \leq 0.867$ . Taking the pressure  $P = 0.01$  for  $k = 1$ , we plot  $\tau - r_+$ , for different values of Gauss-Bonnet coupling  $\alpha$  for  $\varphi = 0.5$  and  $\varphi = 0.9$  in ??.

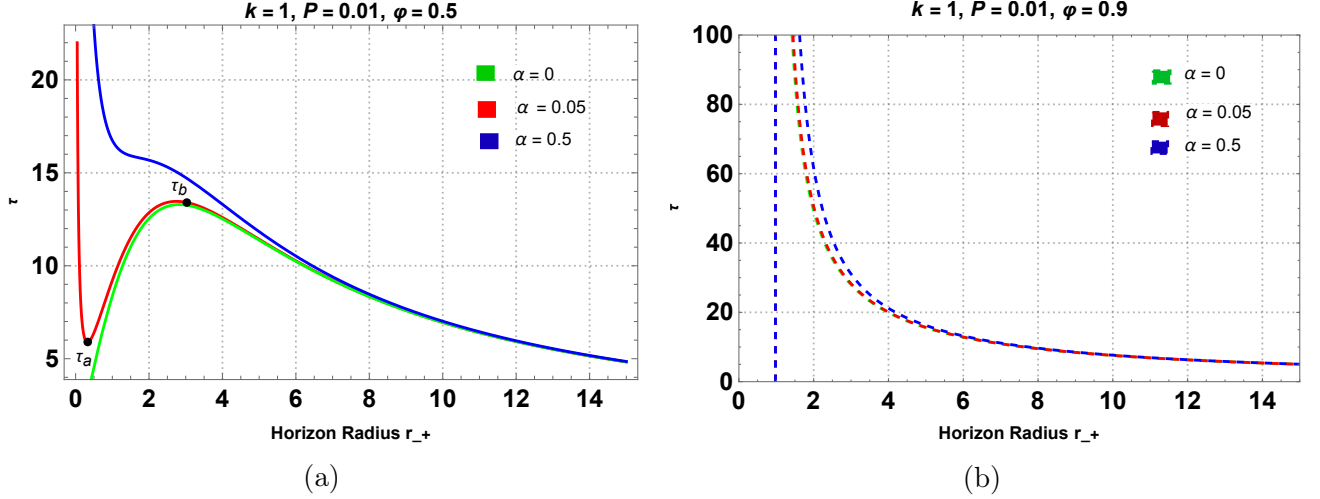


Figure 4: The zero points of  $\phi^{r_+}$  in  $\tau$  vs  $r_+$  plane for charged AdS black hole in grand canonical ensemble with  $\tau = 10$  and pressure  $P = 0.01$ . Here for (a)  $\varphi = 0.5$ , for (b)  $\varphi = 0.9$

When  $\varphi = 0.5$  (see Figure 4a), we observe two black hole branches for RN black holes ( $\alpha = 0$ ), three black hole branches for  $\alpha = 0.05$ , and only one black hole branch for  $\alpha = 0.5$ , whereas for  $\varphi = 0.9$  (see Figure 4b), we only have one black hole branch for all values of  $\alpha$ . We calculate the winding number as well as the topological number for each solution case by case. In the Table 2, we provide the number of zero points for various parameters for the spherical black hole ( $k = 1$ ). We will discuss each case separately.

*Case 1-  $\alpha = 0$ :* for  $\tau = 10$ ,  $\varphi = 0.5$ , and  $P = 0.01$ , we find two zero points  $ZP_1$  and  $ZP_2$  with winding numbers  $-1$  and  $1$  respectively. These are shown in Figure 5a. Hence, the topological number is  $W = +1 - 1 = 0$  for RN AdS black holes in the grand canonical ensemble, which differs from the case in the canonical ensemble. Black holes with winding number  $w = -1$  represent unstable black holes while regions with zero points with winding number  $w = 1$  represent stable black holes. We repeated this analysis for the higher value of pressure  $P$  as well and we found that the topological number remains  $W = 0$ .

Interestingly, however for potential values  $\varphi > 0.86$ , we get only one black hole branch with

Case $k = 1$		$P = 0.01$	# of ZP
$\alpha = 0$	$\tau$	1 – 13	2
$\varphi = 0.5$		14 – $\tau_{max}$	-
$\alpha = 0.05$	$\tau$	1 – 5.5	1
		5.5 – 13.5	3
$\varphi = 0.5$		13.5 – $\tau_{max}$	1
$\alpha = 0.5$	$\tau$	1 – $\tau_{max}$	1
$\varphi = 0.5$			

Table 2: Zero points of spherical ( $k=1$ ) Gauss-Bonnet charged AdS black holes for various Gauss-Bonnet coupling in the grand canonical ensemble.

winding number  $w = +1$  as shown in Figure 5b, therefore having topological number  $W = 1$ , the same as the canonical ensemble.

*Case 2-  $\alpha = 0.05$ :* On comparing the red and green curve in Figure 4a, we notice a new phase of stable small black holes and unstable intermediate black hole branch appears as we slightly increase the Gauss-Bonnet coupling. Consequently, three distinct black hole branches are seen for RN black holes with small GB parameter  $\alpha = 0.05$ . This is captured by the increase in the number of zero points <sup>6</sup>. As an example, we illustrate the representation of the unit vectors along with the zero points for GB coupling  $\alpha = 0.05$  in Figure 6.

Using the formula from the previous section, we compute the winding and topological numbers corresponding to these zero points. For example, setting  $\varphi = 0.5$ ,  $k = 1$ ,  $P = 0.01$  and  $\tau = 4.8$ , we can find one zero point ( $ZP_1$ ) as shown in Figure 6a, located at  $(r_0, \Theta) = (15.1, \pi/2)$ . The winding number corresponding to this zero point is found to be  $w = +1$ . Using the same charge and pressure setup, we can locate three zero points:  $ZP_2$ ,  $ZP_3$ , and  $ZP_4$  for  $\tau = 8.6$  with winding numbers of  $+1$ ,  $-1$ , and  $+1$ , respectively. You may view these in Figure 6b. On the other hand, for  $\tau = 13.8$  the system indicates the presence of a single zero point  $ZP_5$  with winding number  $+1$  as shown in Figure 6c.

The red curve in Figure 4a reveals three distinct black hole branches for  $P = 0.01$  when pressure is less than its critical value with  $\tau > \tau_b$  representing the small black hole region. Any zero point on this branch has a winding number of  $w = +1$ . Likewise, for every zero point

<sup>6</sup>So, the number of the solutions of the equation  $\phi^{r+} = 0$  in a fixed  $\tau$  is equal to the number of on-shell black holes in a fixed temperature i.e., the number of black hole branches is the same as the number of zero point of  $\phi^a$  in the  $r_+ - \Theta$  plane.



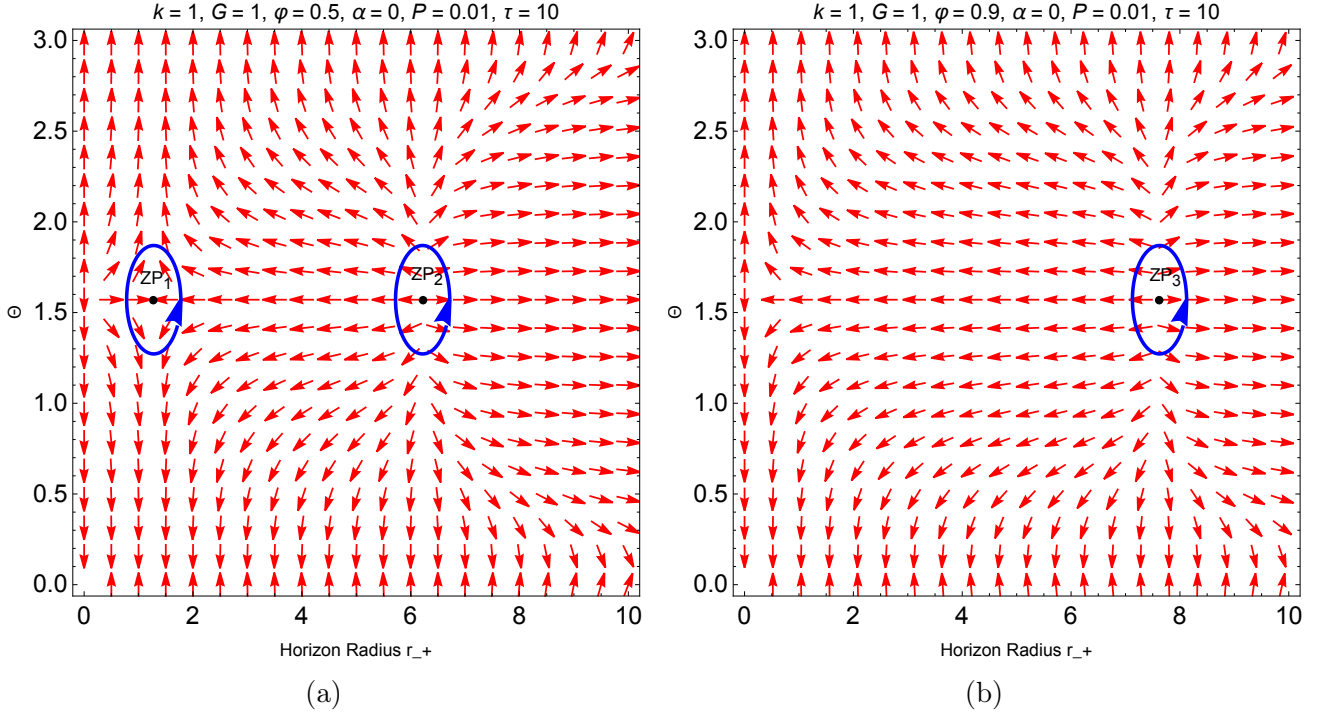


Figure 5: The unit vectors  $(n^1, n^2)$  in  $\Theta$  vs  $r_+$  plane for charged AdS black hole in grand canonical ensemble with  $\tau = 10$  and pressure  $P = 0.01$ . Here for (a)  $\varphi = 0.5$ , for (b)  $\varphi = 0.9$ .

on the large black hole region  $\tau < \tau_a$ , the winding number  $w = +1$  is noted. In the region  $\tau_a < \tau < \tau_b$  there are three black hole branches, since we find that the small and large black hole branches have  $w = 1$ , it implies that the winding number of the intermediate black hole branch is  $w = -1$ . Consequently, the topological number is  $W = +1 - 1 + 1 = +1$ . This is the same as the canonical ensemble. In section 4, we explicitly calculate the specific heat at each of the three branches and show that the branches with winding numbers of  $+1$  and  $-1$  have positive and negative specific heat, respectively, indicating thermodynamic stability and instability. We checked that above critical pressure  $P > P_c$ , the unstable intermediate region disappears and  $\tau(r_+)$  curve shows one stable black hole branch with  $+1$  winding number for each point on the curve and hence, the topological number remains  $+1$ .

*Case 3-  $\alpha = 0.5$ :* From (3.1.8), we know as the coupling  $\alpha$  increases, the critical value of pressure  $P_c$  decreases. For  $\alpha = 0.5$  and  $\varphi = 0.5$ , the critical pressure is found to be  $P_c = 0.008$ . Like  $\alpha = 0.05$ , in Figure 7a, the red curve reveals three distinct black hole branches for  $P = 0.001$ , and the blue curve represents only one black hole branch, leaving one zero point for  $P = 0.01$  which is shown in  $\Theta$  vs  $r_+$  plane in Figure 7b.

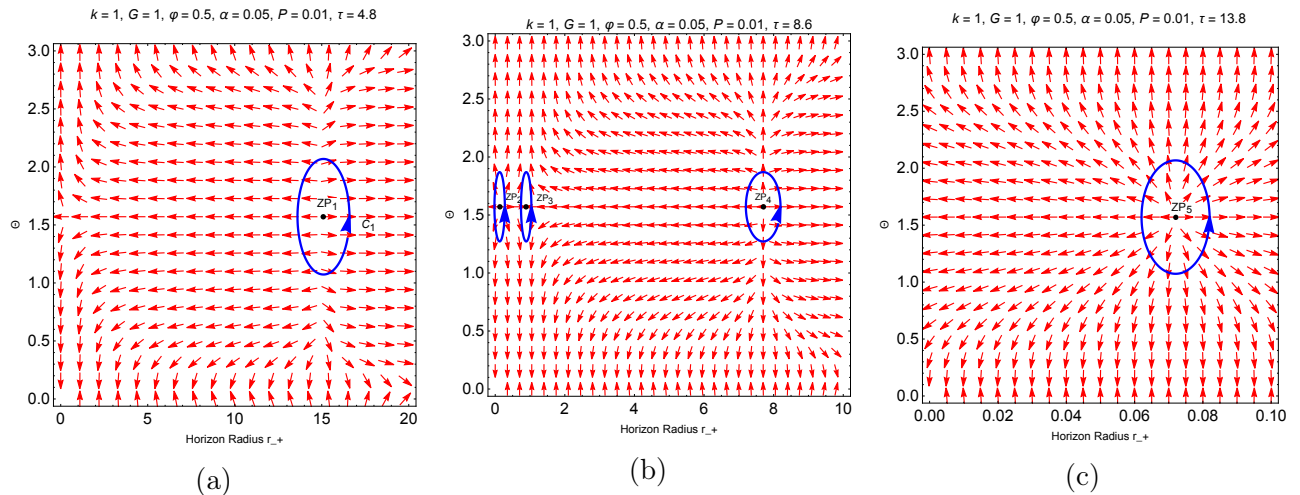


Figure 6: The unit vectors  $(n^1, n^2)$  in  $\Theta$  vs  $r_+$  plane for charged Gauss-Bonnet AdS black hole in grand canonical ensemble with coupling  $\alpha = 0.05$  and pressure less than the critical value. Here for (a)  $\tau = 4.8$ , for (b)  $\tau = 8.6$  and for (c)  $\tau = 13.8$

### 3.2.3 $k = -1$

The zero-point solution for hyperbolic horizon geometry is given as

$$\tau = \frac{6\pi (r_+^2 - 2\alpha)}{r_+ (8\pi P r_+^2 - 4\varphi^2 - 3)}. \quad (3.2.8)$$

From (2.0.10), we know that the hyperbolic horizon radius must be  $r_+^2 \geq 6\alpha$ . We also found that the hyperbolic-charged AdS black hole in the grand canonical ensemble does not have any critical points. In Figure 8, we observe that irrespective of the GB parameter  $\alpha$  and potential  $\varphi$ , we get one stable black hole branch. For a system with  $\alpha = 0.05$ ,  $\varphi = 0.5$ ,  $P = 0.01$  and  $\tau = 5$ , we found one zero point with winding number  $+1$ , as shown in Figure 8c. Hence, the topological number of hyperbolic-RN GB AdS black holes in the grand canonical ensemble is  $+1$ . Upon repeating the studies for various pressure variations, we discovered that the topological number( $+1$ ) remains unchanged.

## 4 Stability and Phase transition of RN GB Topological Black Holes

We now explore the thermodynamic stability and phase structure of the black hole solutions by conventional methods i.e., to determine the local stability of the black hole, we calculate the

Case $k = 1$ $\alpha = 0.05, \varphi = 0.5$	Number of Zero Points	Winding number	Topological Number $\sum w_i = W$
Case 1: $\tau < \tau_a$	1	$w _{\text{ZP}_1} = 1$	1
Case 2: $\tau_a < \tau < \tau_b$	3	$w _{\text{ZP}_2} = +1$ $w _{\text{ZP}_3} = -1$ $w _{\text{ZP}_4} = +1$	1
Case 3: $\tau > \tau_b$	1	$w _{\text{ZP}_1} = 1$	1

Table 3: The zero points for  $\alpha = 0.05$  and pressure less than the critical value, where  $\tau_a = 5.5$  and  $\tau_b = 13.5$ .

specific heat with the fixed chemical potential and use its sign to determine the stability of the black hole as a thermodynamic system in a grand canonical ensemble. The black hole is stable over the whole temperature range if the specific heat is always positive. The temperature  $T$  of an RN GB black hole in the grand canonical ensemble is expressed as a function of pressure  $P$ , horizon radius, and electric potential  $\varphi$  as

$$T = \frac{r_+ (3k + 8\pi P r_+^2 - 4\varphi^2)}{6\pi (r_+^2 + 2k\alpha)}. \quad (4.0.1)$$

In Figure 9 and Figure 10, we plot temperature as a function of horizon radius for  $k = -1, 0, 1$  with pressure below critical and above its critical value, respectively. We make the following observations :

- When  $\alpha = 0$ , the temperature starts at zero and monotonically increases for the cases  $k = 0$  and  $-1$ . However, for spherical horizon  $k = 1$ , the behavior of the temperature depends on the potential.
- In the presence of non-zero GB parameter  $\alpha$ , we observe that thermodynamical quantities depend on the potential  $\varphi$ , parameter  $\alpha$ , and non-zero horizon structure  $k$ .
- The Presence of potential only influences the temperature behavior when the horizon radius is small.
- On increasing the pressure above its critical value, the intermediate black phase of RN AdS with Gauss-Bonnet coincides and we are left with only one black hole phase.

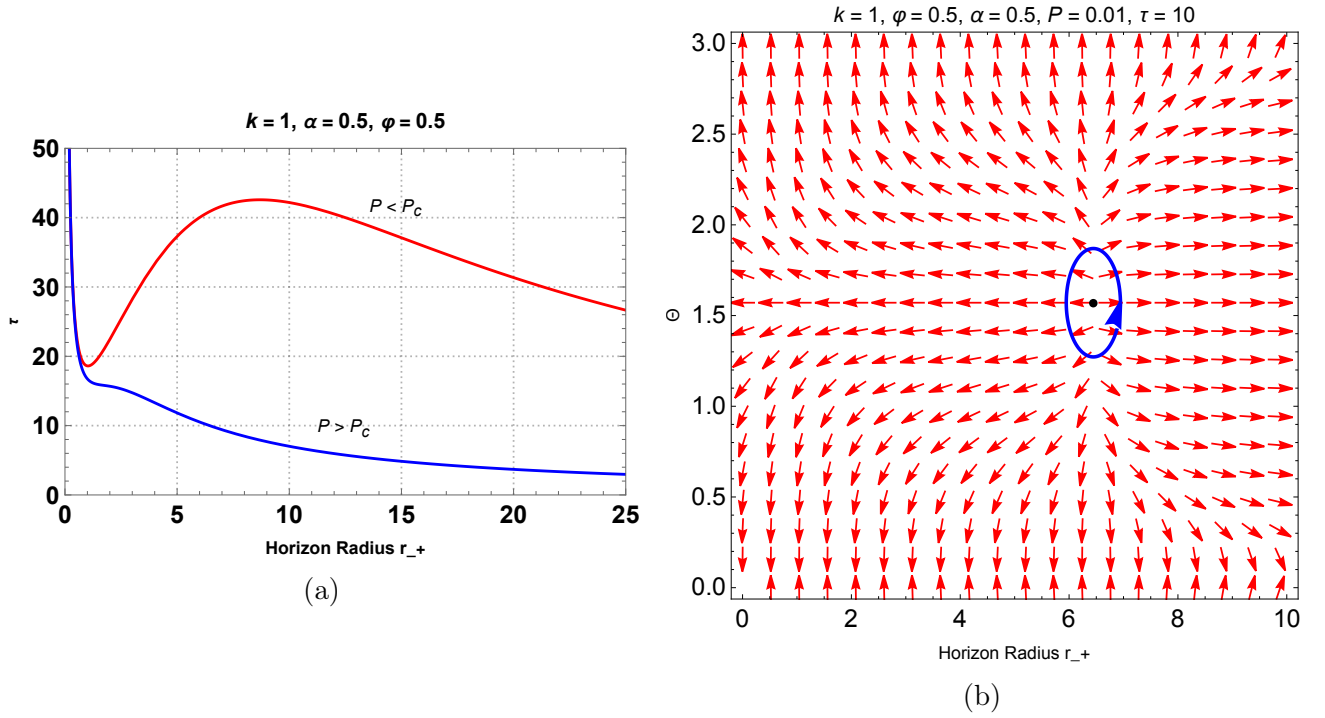


Figure 7: (a) The zero points of  $\phi^{r_+}$  in  $\tau$  vs  $r_+$  plane for  $P = 0.001 < P_c$  (red) and  $P = 0.01 > P_c$  (blue). (b) The unit vectors  $(n^1, n^2)$  in  $\Theta$  vs  $r_+$  plane, for coupling  $\alpha = 0.5$  and pressure  $P = 0.01$  higher than the critical value.

## 4.1 Local Stability

The specific heat serves as the foundation for the investigation of local thermodynamic stability. More specifically, it must be strictly positive for it to be considered locally stable to a disturbance in a set of parameters. In this subsection, we systematically compute the specific heat of several thermodynamic systems and determine whether branches with winding numbers of  $+1$  or  $-1$  have positive or negative specific heat. The specific heat for a given potential in a grand canonical ensemble may be computed using the following equation:

$$C_\varphi = T \left( \frac{\partial S}{\partial T} \right)_{P,\varphi} = T \left( \frac{\partial S}{\partial r_+} \right)_{P,\varphi} \left( \frac{\partial r_+}{\partial T} \right)_{P,\varphi}. \quad (4.1.1)$$

By using the equation of entropy (2.0.7), we obtain

$$\left( \frac{\partial S}{\partial r_+} \right)_{P,\varphi} = \frac{3\pi^2 (r_+^2 + 2\alpha k)}{2} > 0. \quad (4.1.2)$$

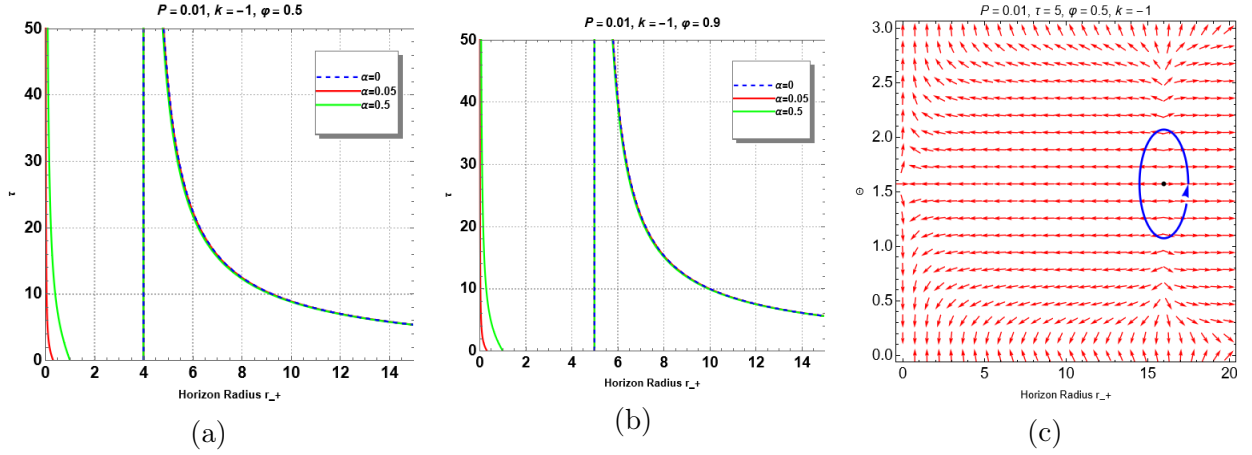


Figure 8: The zero points of  $\phi^{r_+}$  in  $\tau$  vs  $r_+$  plane for hyperbolic charged AdS black hole in grand canonical ensemble with  $\tau = 10$  and pressure  $P = 0.01$ . Here for (a)  $\varphi = 0.5$ , for (b)  $\varphi = 0.9$  (c) The unit vectors  $(n^1, n^2)$  in  $\Theta$  vs  $r_+$  plane for hyperbolic charged Gauss-Bonnet AdS black hole in grand canonical ensemble with coupling  $\alpha = 0.05$ ,  $\tau = 5$ .

The constraint (2.0.10) ensures that the  $(\partial_{r_+} S)_P$  always remains positive. This implies that the sign of specific heat is the same as the sign of  $(\partial_{r_+} T)_P$

$$C_\varphi = - \frac{3\pi^2 r_+ (r_+^2 + 2k\alpha)^2 (3k + 8P\pi r_+^2 - 4\varphi^2)}{2(8k\alpha\varphi^2 - 4r_+^2(2\pi P r_+^2 + \varphi^2) - 6k^2\alpha + k r_+^2(3 - 48\pi\alpha P))}. \quad (4.1.3)$$

#### 4.1.1 $k = 0$

As mentioned in subsection 3.2.1, the expressions of thermodynamic quantities are the same of RN AdS and RN-GB AdS black holes for case  $k = 0$ . The specific heat of RN-GB AdS black hole for this case in grand canonical ensemble is given as

$$C_\varphi = \frac{3\pi^2 r_+^3 (2\pi P r_+^2 - \varphi^2)}{2(2\pi P r_+^2 + \varphi^2)}. \quad (4.1.4)$$

It is evident right away that the RN-GB AdS black holes for the case  $k = 0$  are locally stable over the whole temperature range since the specific heat is always positive. In the topology thermodynamic study subsection 3.2.1, we found one black hole branch for  $k = 0$  with the winding number  $+1$  as shown in Figure 3. This confirms that the branch with a positive winding number has a positive specific heat and thus is thermodynamically stable.

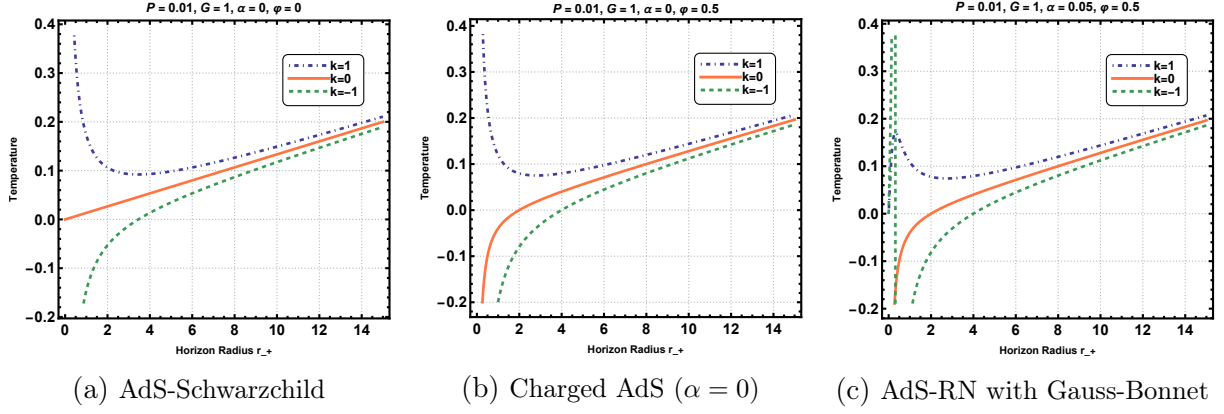


Figure 9: Plot of temperature vs horizon radius  $r_+$  for various values of parameters for  $P < P_c$ .

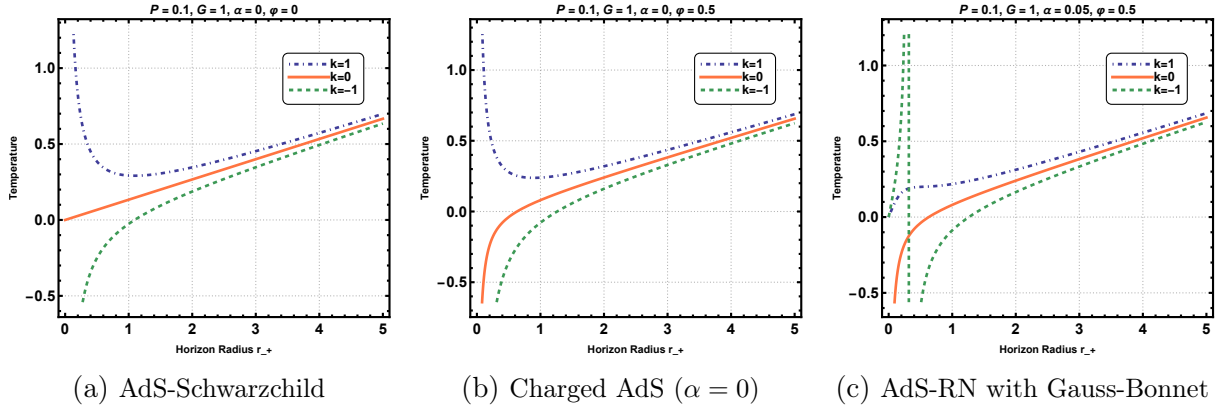


Figure 10: Plot of temperature vs horizon radius  $r_+$  for various values of parameters for  $P > P_c$ .

#### 4.1.2 $k = 1$

The specific heat of spherical RN GB AdS black hole ( $k = 1$ ) in grand canonical ensemble is given as

$$C_\varphi = \frac{3\pi^2 r_+ (r_+^2 + 2\alpha)^2 (8\pi P r_+^2 - 4\varphi^2 + 3)}{2(\alpha(6 - 8\varphi^2) + 8\pi P r_+^4 + r_+^2(48\pi\alpha P + 4\varphi^2 - 3))}. \quad (4.1.5)$$

In Figure 13 and Figure 14, we present the plot for specific Heat  $C_\varphi$  versus horizon radius  $r_+$  for various potential values with Gauss-Bonnet coupling ( $\alpha = 0, \alpha = 0.05$ , and  $\alpha = 0.5$ ) for pressure  $P = 0.01$  and  $P = 0.1$ , respectively.

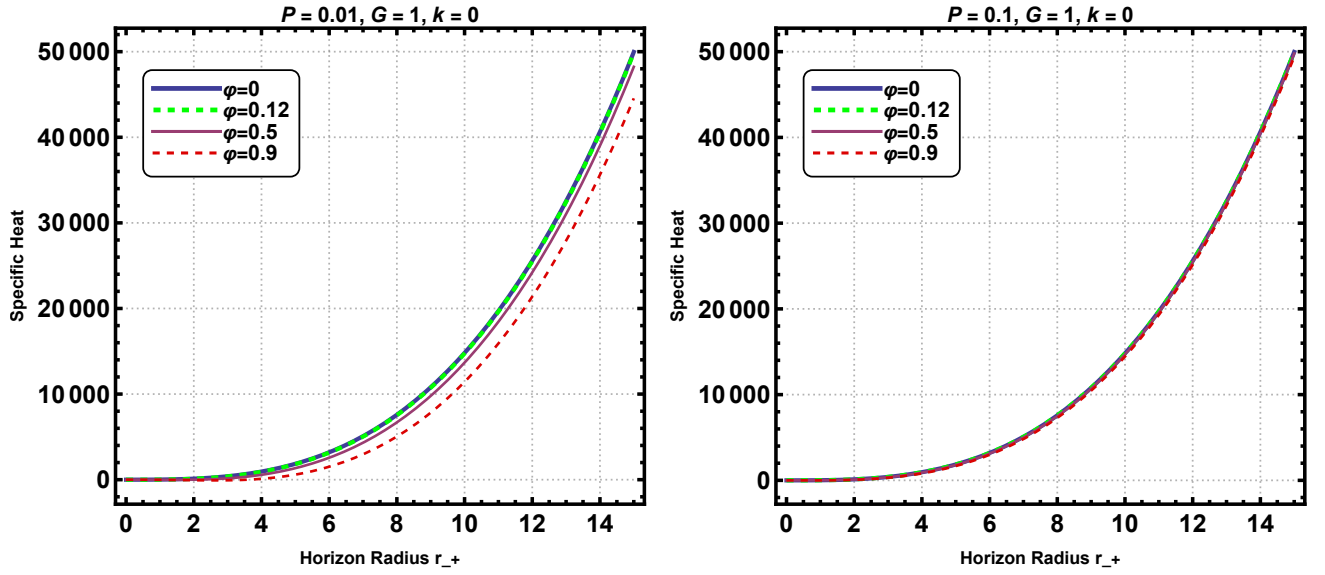


Figure 11: Specific Heat vs Horizon radius for  $k = 0$  with for different parameters.

### 4.1.3 $k = -1$

The specific heat of hyperbolic RN-GB AdS black hole for the case  $k = -1$  in grand canonical ensemble

$$C_\varphi = \frac{3\pi^2 r_+ (r_+^2 - 2\alpha)^2 (8\pi P r_+^2 - 4\varphi^2 - 3)}{2(8\pi P r_+^4 + r_+^2 (4\varphi^2 - 48\pi\alpha P + 3) + 2\alpha (4\varphi^2 + 3))}. \quad (4.1.6)$$

Since the specific heat is always positive, it is immediately clear that the RN-GB AdS black holes for case  $k = -1$  are locally stable across the whole temperature range. As seen in subsection 3.2.3, we discovered one black hole branch for negative constant curvature with the winding number +1. This reaffirms that the branch with a positive winding number is thermodynamically stable.

## 4.2 Phase Transition

In the grand canonical ensemble, the gauge potential the chemical potential conjugate to the electric charge—is fixed, and the Gibbs free energy is the corresponding free energy. In the presence of negative Gibbs free energy, the black hole phase predominates over the thermal AdS space phase. This scenario suggests that the black hole is favored universally, or at least

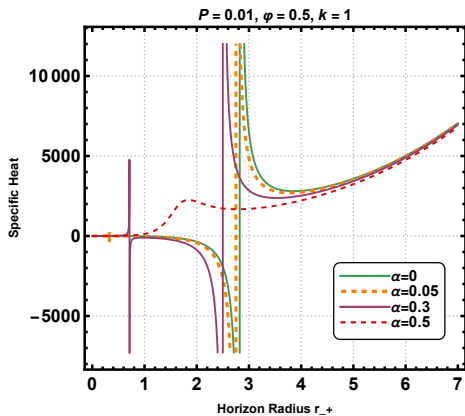


Figure 12: Specific Heat  $C_\varphi$  versus Horizon radius  $r_+$  for  $\varphi = 0.5$  and  $P = 0.01$  for Gauss-Bonnet coupling

In Figure 12, we observe that the smooth transition from small to large black holes is disrupted below the threshold potential value  $\alpha_c$  in the region of intermediate temperatures where three equilibria exist. The specific heat of the small black hole rises while the large black hole falls as the temperature rises in this area. At  $\alpha_c$ , they intersect, making a large black hole universally stable. In subsection 3.2, these phenomenon is captured by changing the number of zero points.

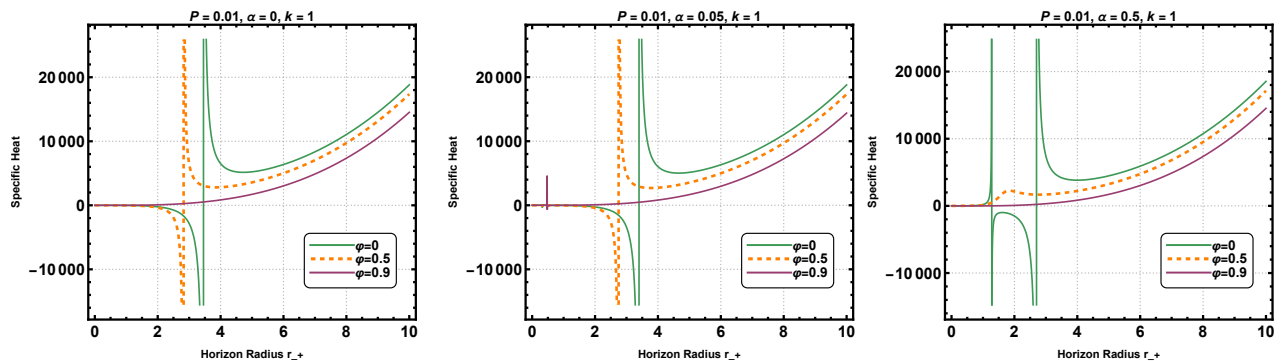


Figure 13: In the grand canonical ensemble for  $k = 1$  and pressure  $P = 0.01$ : Specific Heat  $C_\varphi$  versus Horizon radius  $r_+$  for various potential values with Gauss-Bonnet coupling ( $\alpha = 0, \alpha = 0.05, \text{ and } \alpha = 0.5$ ).

globally stable. Nevertheless, the Hawking-Page phase transition between the thermal AdS space and the AdS black hole happens when the sign of the Gibbs free energy changes. We make following observations from Figure 17 and Figure 18:

1. When  $\alpha = 0$ , the free energy starts at zero and remains negative for the cases  $k = 0$  and  $-1$ . However, for spherical horizon  $k = 1$ , the behavior of the free energy depends on the potential  $\varphi$ .
2. In the presence of non-zero GB parameter  $\alpha$ , we know from condition (2.0.10) that the horizon radius  $r_+^2 > 6\alpha$  is bounded from below for the hyperbolic horizon. Thus, the free energy for the cases  $k = 0$  and  $-1$  remains negative for the allowed horizon radius.



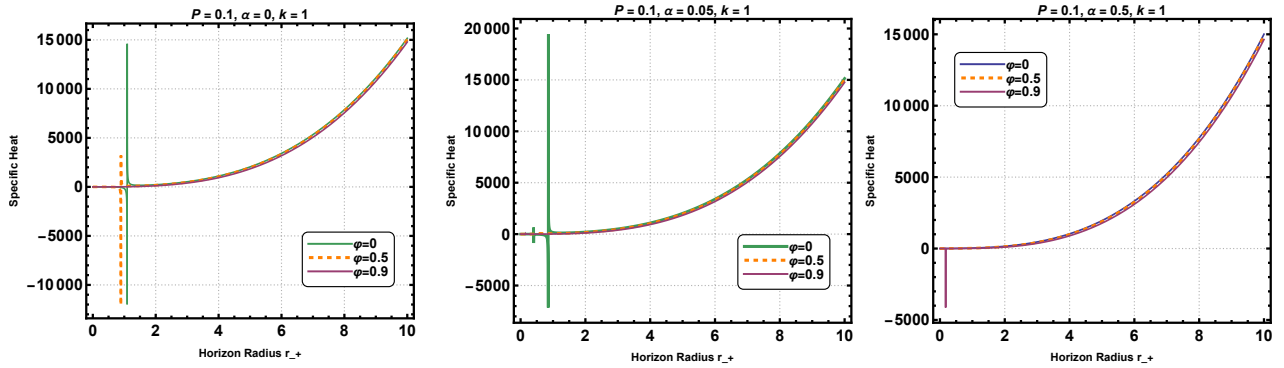


Figure 14: In the grand canonical ensemble for pressure higher than critical value  $P = 0.1$ : Specific Heat  $C_\Phi$  versus Horizon radius  $r_+$  for various potential values with Gauss-Bonnet coupling ( $\alpha = 0, \alpha = 0.05$ , and  $\alpha = 0.5$ ).

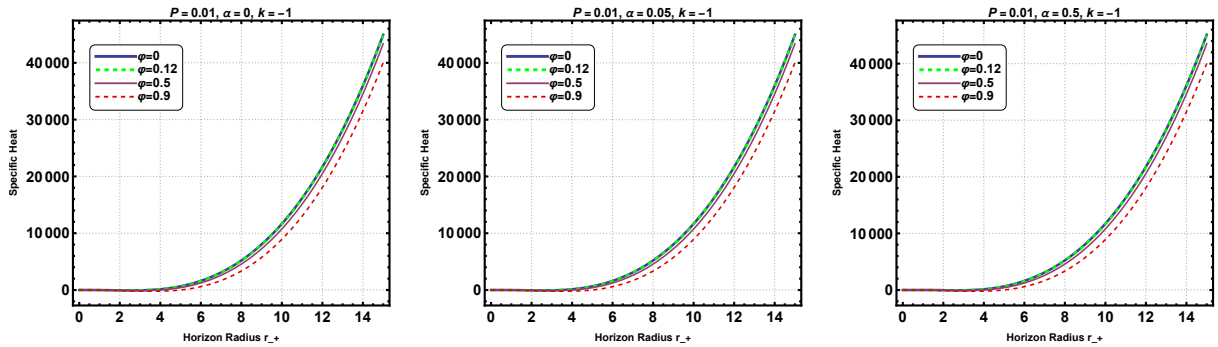


Figure 15: Specific Heat vs. Horizon radius in the grand canonical ensemble for  $k = -1$  and  $P = 0.01$  for potential values. Here (a)  $\alpha = 0$ , (b)  $\alpha = 0.05$ , and (c)  $\alpha = 0.5$ .

3. The interesting system is  $k = 1$ , the sign of free energy in this system changes depending on the potential  $\varphi$  and parameter  $\alpha$ .
4. Even on increasing the pressure above its critical value, the black holes for the cases  $k = 0$  and  $-1$  remain stable.
5. The sign of free energy continues to change near a smaller horizon radius in a spherical ( $k = 1$ ) black hole when  $P > P_c$  for RN AdS black holes. Since there is no phase disappearing critical point. On the other hand, the RN GB black holes become stable for all values of horizon radius when  $P > P_c$ .

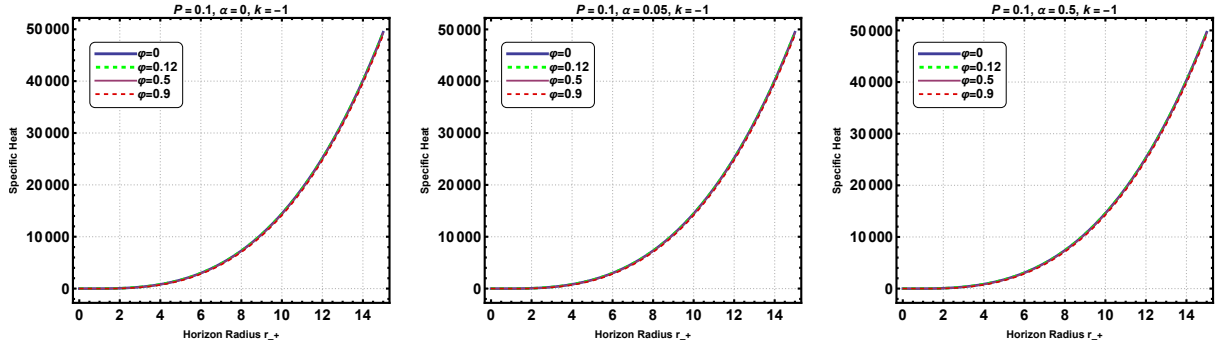


Figure 16: Specific Heat vs Horizon radius in the grand canonical ensemble for  $k = -1$  and  $P = 0.1$  for potential values. Here (a)  $\alpha = 0$ , (b)  $\alpha = 0.05$ , and (c)  $\alpha = 0.5$ .

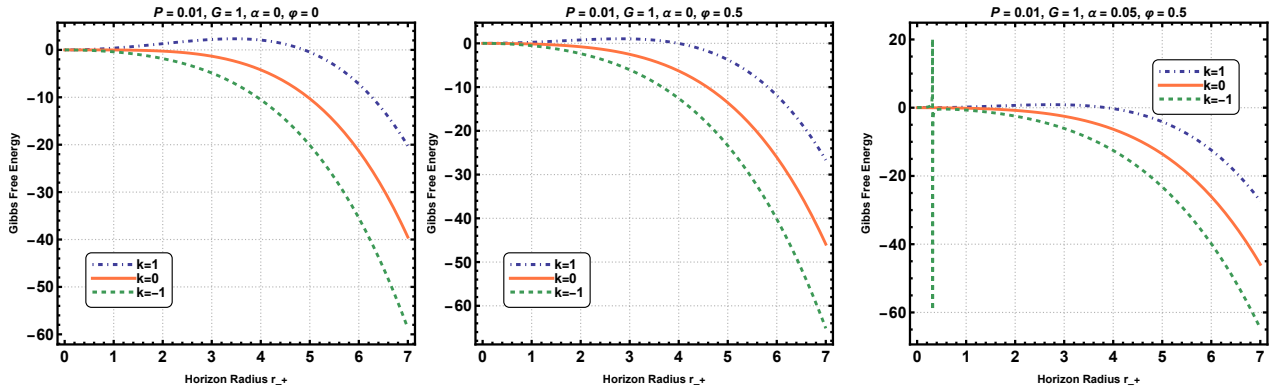


Figure 17: In the grand canonical ensemble: the behavior of Gibbs Free Energy vs horizon radius  $r_+$  for various values of parameters for  $P < P_c$ .

#### 4.2.1 $k = 0$

The temperature  $T$  and on-shell Gibbs free energy  $G$  for  $k = 0$  case in the grand canonical ensemble is given as

$$T = \frac{4Pr_+}{3} - \frac{2\varphi^2}{3\pi r_+}, \quad G = -\frac{1}{6}\pi r_+^2 (\pi P r_+^2 + \varphi^2). \quad (4.2.1)$$

The Figure 19, shows that for  $k = 0$  case there is no phase transition and the black hole remains stable for all parameter values. Thus, we conclude that black holes for such cases are globally stable.

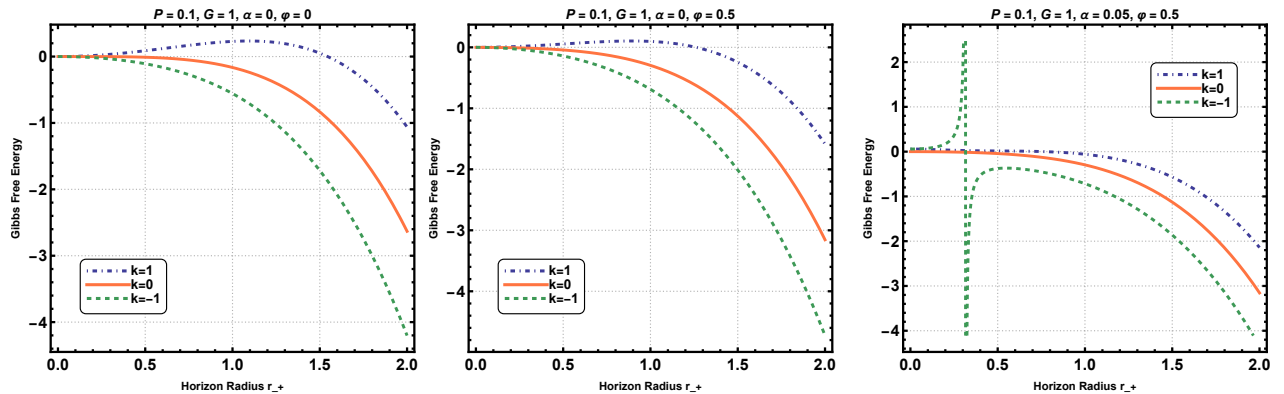


Figure 18: In the grand canonical ensemble: the behavior of Gibbs Free Energy vs horizon radius  $r_+$  for various values of parameters for  $P > P_c$ .

#### 4.2.2 $k = 1$

In the grand canonical ensemble, the temperature  $T$  and on-shell Gibbs free energy  $G$  for spherical RN GB black holes are given as

$$T = \frac{8\pi P r_+^3 - 4r_+ \varphi^2 + 3r_+}{12\pi\alpha + 6\pi r_+^2}, \quad (4.2.2)$$

$$G = \frac{\pi (18\alpha^2 - 4\pi P r_+^6 + r_+^4 (-72\pi\alpha P - 4\varphi^2 + 3) + 3\alpha r_+^2 (8\varphi^2 - 3))}{24(2\alpha + r_+^2)}. \quad (4.2.3)$$

By examining the Gibbs free energy, we see that the solutions display the Hawking-Page (HP) transition between the thermal AdS space and the stable large black holes. Additionally, we discover that below the critical pressure, the solutions exhibit a liquid/gas-like phase change. Within the thermal AdS background, the Gibbs free energy is consistently zero. The HP phase transition occurs when the Gibbs free energy of the black hole-thermal AdS system vanishes. The HP phase transition temperature at vanishing  $G = 0$  is given as

$$T_{HP} = \frac{3\alpha + 4\pi P r_+^4 - 4r_+^2 \varphi^2 + 3r_+^2}{4\pi r_+^3 + 24\pi\alpha r_+}. \quad (4.2.4)$$

From the (4.2.4), we notice that increasing pressure causes the  $T_{HP}$  to rise, while increasing the value of GB parameter  $\alpha$  and electric potential  $\varphi$  causes it to fall. In Figure 20, we plot phase transition for fixed pressure  $P = 0.01$ . For potential  $\varphi = 0.9 > 0.86$  (blue), the black hole does not exhibit a critical phenomenon and we see one stable black hole phase for all parameter values with no first-order phase transition. This is consistent with our topology thermodynamics analysis in Sec.[3.2.2] where for potential values  $\varphi > 0.86$ , we saw only one

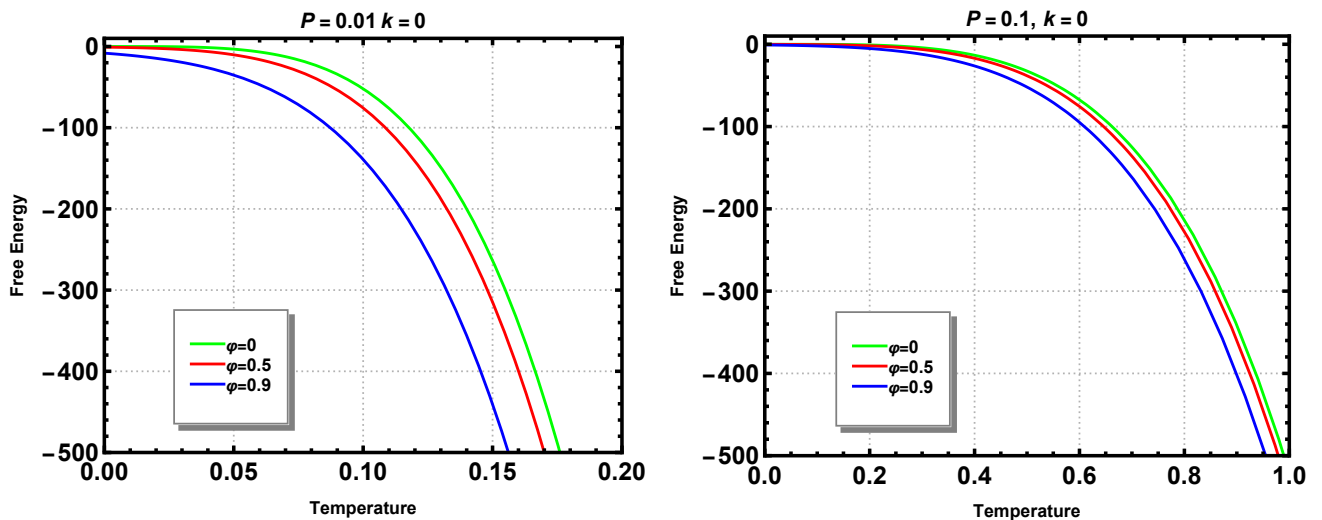


Figure 19: Phase transition for  $k = 0$  with for different parameters.

black hole branch (see Fig5b) with winding number  $w = +1$ . However, for non-zero GB parameter  $\alpha$ , the system does go under Hawking-Page transition at  $G = 0$  and temperature  $T_{HP}$ . Below  $T_{HP}$ , AdS thermal space dominates over black hole solutions. Furthermore, we

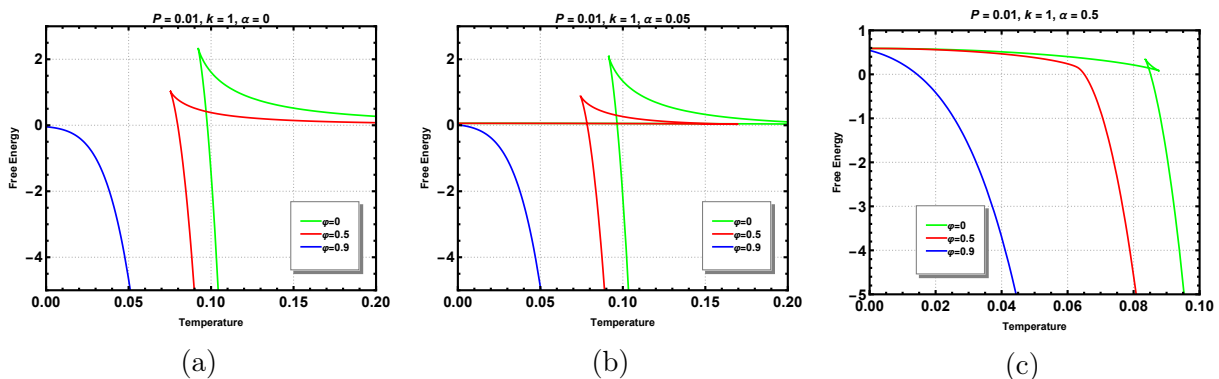


Figure 20: Phase transition in the grand canonical ensemble for  $k = 1$  and  $P = 0.01$  for potential values. Here (a)  $\alpha = 0$ , (b)  $\alpha = 0.05$ , and (c)  $\alpha = 0.5$ .

notice that unlike the blue curve ( $\varphi = 0.9$ ) in Figure 20, the system represented by green ( $\varphi = 0$ ) and red ( $\varphi = 0.5$ ) curve show different phase transitions structure depending on the GB parameter value.

For  $\alpha = 0$ , we witness Hawking-Page transition between the thermal AdS space and RN black holes where phase transition temperature  $T_{HP}$  reduces with increasing value of  $\varphi$ . In the topology thermodynamics, this was captured by unstable black with winding number  $w = -1$

and stable black holes with  $w = 1$ . Hence, for RN AdS black holes have a topological number is  $W = -1 + 1 = 0$ .

For  $\alpha = 0.05$ , the black holes in green ( $\varphi = 0$ ) and red ( $\varphi = 0.5$ ) with pressure  $P = 0.01 < P_c$  have two thermodynamically stable phases and one intermediate thermodynamically unstable phase. Specifically, the swallowtail form indicates that the black hole experiences a first-order phase transition between thermodynamically stable phases. Similarly, for  $\alpha = 0.5$ , the GB AdS black holes (in green  $\varphi = 0$ ) with the pressure  $P = 0.01 < P_c$  show three phases, two stable and one unstable.

However, for  $\alpha = 0.5$ , the RN GB black hole (in red  $\varphi = 0.5$ ) with the  $P = 0.01 > P_c$  does not go under first-order phase transition but they admit HP transition at  $G = 0$ .

### 4.2.3 $k = -1$

In the grand canonical ensemble, the temperature  $T$  and on-shell Gibbs free energy  $G$  for hyperbolic RN-GB black holes are given as

$$T = \frac{r_+ (8\pi P r_+^2 - 4\varphi^2 - 3)}{6\pi (r_+^2 - 2\alpha)}, \quad (4.2.5)$$

$$G = -\frac{\pi (18\alpha^2 + 4\pi P r_+^6 + r_+^4 (-72\pi\alpha P + 4\varphi^2 + 3) + 3\alpha r_+^2 (8\varphi^2 + 3))}{24 (r_+^2 - 2\alpha)}. \quad (4.2.6)$$

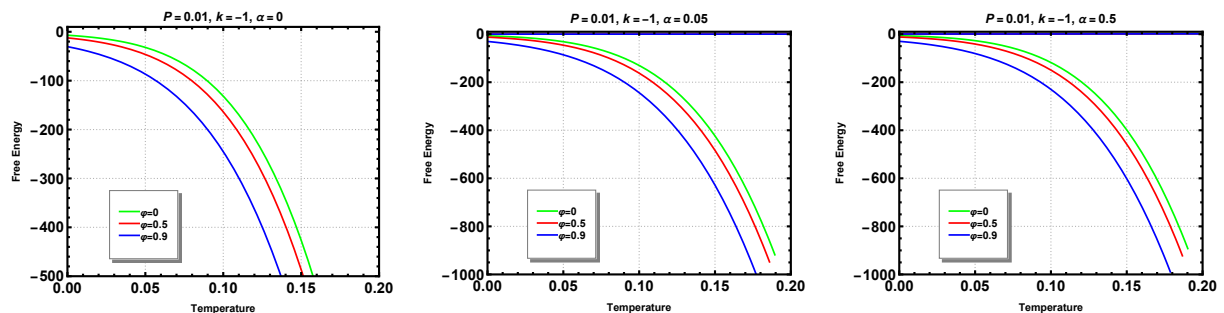


Figure 21: Phase transition in the grand canonical ensemble for  $k = -1$  and  $P = 0.01$  for potential values. Here (a)  $\alpha = 0$ , (b)  $\alpha = 0.05$ , and (c)  $\alpha = 0.5$ .

Similar to the  $k = 0$  case, the Figure 21, shows that for the  $k = -1$  case, there is no phase transition and the black hole remains stable for all parameter values and is globally preferred.

## 5 Conclusion

We have presented topology thermodynamic analysis and conventional phase structure study for five-dimensional charged Gauss-Bonnet black holes in a grand canonical ensemble. We conclude that in the cases  $k = -1$  and  $k = 0$ , the black holes with and without the Gauss-Bonnet coupling have the same thermodynamic properties. For both cases, there are no critical points in the grand canonical ensemble. There exists one stable globally preferred black hole with topological number  $+1$ .

For the case  $k = 1$ , the system exhibits critical behavior for non-zero positive Gauss-Bonnet coupling  $\alpha > 0$  within the potential range  $0 \leq \varphi \leq 0.86$ . There exists one black hole branch when the potential is  $\varphi > 0.86$ , with topological number  $W = +1$ . There occurs the Hawking-Page transition between RN-GB black hole and AdS thermal space for  $\alpha > 0$  and  $\varphi > 0.86$  at  $(G = 0, T_{HP})$ . On the other hand, below critical pressure, for potentials within the range  $0 \leq \varphi \leq 0.86$ , the presence of Gauss-Bonnet coupling in the grand canonical ensemble creates an intermediate unstable black hole phase, which is absent in RN Black hole in the grand canonical ensemble.

In topology thermodynamics black holes are classified into different topological classes based on their topological number. We found that the spherical RN black hole shows two black hole solutions one with winding number  $+1$  (large stable) and one with a  $-1$  (small unstable). Thus, the topological number for RN AdS black holes is  $0$  for all pressure values. Furthermore, in the presence of GB coupling, the RN-GB AdS black hole has three black hole phases for pressure below critical value, two with a  $+1$  winding number (stable small and stable large) and one with a  $-1$  winding number (unstable intermediate phase). However, for pressure above the critical value, there exists one stable solution. The topological number of RN-GB AdS black holes for values of pressure is  $+1$ . We know from previous studies that the topological number for RN AdS and RN-GB AdS black holes in a canonical ensemble is  $+1$ . Thus, we conclude that the RN-GB AdS and RN AdS black holes belong to different topological classes in the grand canonical ensemble. But, the RN AdS and RN-GB AdS black holes in canonical ensemble and RN-GB AdS black holes in grand canonical, belong to the same topological class. We would also like to point out that topological thermodynamics provides innovative methods to categorize various black holes and critical points, but it fails to offer a complete phase structure picture. It gives no information regarding the Hawking-Page phase transition. In summary, traditional approaches to studying black hole thermodynamics are still relevant

and important.

## Acknowledgements

This research was supported by an appointment to the YST Program (MM) and JRG Program at the APCTP through the Science and Technology Promotion Fund and Lottery Fund of the Korean Government, by the Korean Local Governments - Gyeongsangbuk-do Province and Pohang City, and by the National Research Foundation of Korea (NRF) grant funded by the Korean government (MSIT) (No. 2021R1F1A1048531). B.-H. Lee (2020R1F1A1075472) and W. Lee (2022R1I1A1A01067336) and CQUeST (Grant No. 2020R1A6A1A03047877) were supported by the Basic Science Research Program through the National Research Foundation of Korea is funded by the Ministry of Education. We wish to thank Alfredo González Lezcano, Augniva Ray for many interesting and useful discussions related to the topics discussed in this paper.

## References

- [1] S. W. Hawking and D. N. Page, *Thermodynamics of Black Holes in anti-De Sitter Space*, *Commun. Math. Phys.* **87** (1983) 577.
- [2] H. W. Braden, J. D. Brown, B. F. Whiting and J. W. York, Jr., *Charged black hole in a grand canonical ensemble*, *Phys. Rev. D* **42** (1990) 3376.
- [3] A. Chamblin, R. Emparan, C. V. Johnson and R. C. Myers, *Charged AdS black holes and catastrophic holography*, *Phys. Rev. D* **60** (1999) 064018 [[hep-th/9902170](#)].
- [4] A. Chamblin, R. Emparan, C. V. Johnson and R. C. Myers, *Holography, thermodynamics and fluctuations of charged AdS black holes*, *Phys. Rev. D* **60** (1999) 104026 [[hep-th/9904197](#)].
- [5] T. K. Dey, S. Mukherji, S. Mukhopadhyay and S. Sarkar, *Phase Transitions in Higher Derivative Gravity*, *JHEP* **04** (2007) 014 [[hep-th/0609038](#)].
- [6] T. K. Dey, S. Mukherji, S. Mukhopadhyay and S. Sarkar, *Phase transitions in higher derivative gravity and gauge theory: R-charged black holes*, *JHEP* **09** (2007) 026 [[0706.3996](#)].

- [7] D. Anninos and G. Pastras, *Thermodynamics of the Maxwell-Gauss-Bonnet anti-de Sitter Black Hole with Higher Derivative Gauge Corrections*, *JHEP* **07** (2009) 030 [0807.3478].
- [8] D.-C. Zou, Y. Liu and B. Wang, *Critical behavior of charged Gauss-Bonnet AdS black holes in the grand canonical ensemble*, *Phys. Rev. D* **90** (2014) 044063 [1404.5194].
- [9] H. Abdusattar, *Stability and Hawking-Page-like phase transition of phantom AdS black holes*, *Eur. Phys. J. C* **83** (2023) 614.
- [10] S.-W. Wei and Y.-X. Liu, *Topology of black hole thermodynamics*, *Phys. Rev. D* **105** (2022) 104003 [2112.01706].
- [11] Y. Duan, *THE STRUCTURE OF THE TOPOLOGICAL CURRENT*, .
- [12] P. K. Yerra and C. Bhamidipati, *Topology of black hole thermodynamics in Gauss-Bonnet gravity*, *Phys. Rev. D* **105** (2022) 104053 [2202.10288].
- [13] S.-W. Wei, Y.-X. Liu and R. B. Mann, *Black Hole Solutions as Topological Thermodynamic Defects*, *Phys. Rev. Lett.* **129** (2022) 191101 [2208.01932].
- [14] J. W. York, Jr., *Black hole thermodynamics and the Euclidean Einstein action*, *Phys. Rev. D* **33** (1986) 2092.
- [15] S.-W. Wei, Y.-X. Liu and Y.-Q. Wang, *Dynamic properties of thermodynamic phase transition for five-dimensional neutral Gauss-Bonnet AdS black hole on free energy landscape*, *Nucl. Phys. B* **976** (2022) 115692 [2009.05215].
- [16] C. Liu and J. Wang, *Topological natures of the Gauss-Bonnet black hole in AdS space*, *Phys. Rev. D* **107** (2023) 064023 [2211.05524].
- [17] Y. M. Cho and I. P. Neupane, *Anti-de Sitter black holes, thermal phase transition and holography in higher curvature gravity*, *Phys. Rev. D* **66** (2002) 024044 [hep-th/0202140].
- [18] R.-G. Cai, S. P. Kim and B. Wang, *Ricci flat black holes and Hawking-Page phase transition in Gauss-Bonnet gravity and dilaton gravity*, *Phys. Rev. D* **76** (2007) 024011 [0705.2469].



- [19] Y. S. Myung, Y.-W. Kim and Y.-J. Park, *Thermodynamics of Gauss-Bonnet black holes revisited*, *Eur. Phys. J. C* **58** (2008) 337 [0806.4452].
- [20] M. Eune, W. Kim and S.-H. Yi, *Hawking-Page phase transition in BTZ black hole revisited*, *JHEP* **03** (2013) 020 [1301.0395].
- [21] S. Khimphun, B.-H. Lee and W. Lee, *Phase transition for black holes in dilatonic Einstein-Gauss-Bonnet theory of gravitation*, *Phys. Rev. D* **94** (2016) 104067 [1605.07377].
- [22] B.-Y. Su, Y.-Y. Wang and N. Li, *The Hawking-Page phase transitions in the extended phase space in the Gauss-Bonnet gravity*, *Eur. Phys. J. C* **80** (2020) 305 [1905.07155].
- [23] N. Kumar, S. Sen and S. Gangopadhyay, *Phase transition structure and breaking of universal nature of central charge criticality in a Born-Infeld AdS black hole*, *Phys. Rev. D* **106** (2022) 026005 [2206.00440].
- [24] H. Eom, S. Jung and W. Kim, *Hawking-Page phase transition of the Schwarzschild AdS black hole with the effective Tolman temperature*, *JCAP* **09** (2022) 053 [2205.09938].
- [25] P. K. Yerra, C. Bhamidipati and S. Mukherji, *Topology of critical points and Hawking-Page transition*, *Phys. Rev. D* **106** (2022) 064059 [2208.06388].
- [26] R. Li, C. Liu, K. Zhang and J. Wang, *Topology of the landscape and dominant kinetic path for the thermodynamic phase transition of the charged Gauss-Bonnet-AdS black holes*, *Phys. Rev. D* **108** (2023) 044003 [2302.06201].
- [27] R. Li and J. Wang, *Generalized free energy landscapes of charged Gauss-Bonnet-AdS black holes in diverse dimensions*, *Phys. Rev. D* **108** (2023) 044057 [2304.03425].
- [28] H. Wang and Y.-Z. Du, *Topology of the charged AdS black hole in restricted phase space*, 2406.08793.
- [29] R.-G. Cai, *Gauss-Bonnet black holes in AdS spaces*, *Phys. Rev. D* **65** (2002) 084014 [hep-th/0109133].
- [30] T. Torii and H. Maeda, *Spacetime structure of static solutions in Gauss-Bonnet gravity: Charged case*, *Phys. Rev. D* **72** (2005) 064007 [hep-th/0504141].

- [31] G. W. Gibbons and S. W. Hawking, *Action Integrals and Partition Functions in Quantum Gravity*, *Phys. Rev. D* **15** (1977) 2752.
- [32] S. W. Hawking and S. F. Ross, *Duality between electric and magnetic black holes*, *Phys. Rev. D* **52** (1995) 5865 [[hep-th/9504019](#)].
- [33] S. C. Davis, *Generalized Israel junction conditions for a Gauss-Bonnet brane world*, *Phys. Rev. D* **67** (2003) 024030 [[hep-th/0208205](#)].
- [34] Y. Brihaye and E. Radu, *Black objects in the Einstein-Gauss-Bonnet theory with negative cosmological constant and the boundary counterterm method*, *JHEP* **09** (2008) 006 [[0806.1396](#)].
- [35] D. Kastor, S. Ray and J. Traschen, *Enthalpy and the Mechanics of AdS Black Holes*, *Class. Quant. Grav.* **26** (2009) 195011 [[0904.2765](#)].
- [36] B. P. Dolan, *The cosmological constant and the black hole equation of state*, *Class. Quant. Grav.* **28** (2011) 125020 [[1008.5023](#)].
- [37] B. P. Dolan, *Pressure and volume in the first law of black hole thermodynamics*, *Class. Quant. Grav.* **28** (2011) 235017 [[1106.6260](#)].
- [38] D. Kubiznak and R. B. Mann, *P-V criticality of charged AdS black holes*, *JHEP* **07** (2012) 033 [[1205.0559](#)].
- [39] S.-W. Wei and Y.-X. Liu, *Triple points and phase diagrams in the extended phase space of charged Gauss-Bonnet black holes in AdS space*, *Phys. Rev. D* **90** (2014) 044057 [[1402.2837](#)].
- [40] M. Cvetic, S. Nojiri and S. D. Odintsov, *Black hole thermodynamics and negative entropy in de Sitter and anti-de Sitter Einstein-Gauss-Bonnet gravity*, *Nucl. Phys. B* **628** (2002) 295 [[hep-th/0112045](#)].
- [41] S. Nojiri and S. D. Odintsov, *(Anti-) de Sitter black holes in higher derivative gravity and dual conformal field theories*, *Phys. Rev. D* **66** (2002) 044012 [[hep-th/0204112](#)].
- [42] T. Clunan, S. F. Ross and D. J. Smith, *On Gauss-Bonnet black hole entropy*, *Class. Quant. Grav.* **21** (2004) 3447 [[gr-qc/0402044](#)].

- [43] P. K. Yerra and C. Bhamidipati, *Topology of black hole thermodynamics in gauss-bonnet gravity*, *Phys. Rev. D* **105** (2022) 104053.